Surface incommensurate structure in an anisotropic model with competing interactions on semi-infinite triangular lattice

1997 J. Phys. A: Math. Gen. 30 4187

(http://iopscience.iop.org/0305-4470/30/12/010)

J. Phys. A: Math. Gen. **30** (1997) 4187–4198. Printed in the UK PII: S0305-4470(97)79170-4

Surface incommensurate structure in an anisotropic model with competing interactions on semi-infinite triangular lattice

Pavol Pajerský and Anton Šurda†

Institute of Physics, Slovak Academy of Science, Dúbravská cesta 9, 842 28 Bratislava, Slovakia

Received 28 October 1996

Abstract. An anisotropic spin model on a triangular semi-infinite lattice with ferromagnetic nearest-neighbour interactions and one antiferromagnetic next-nearest-neighbour interaction is investigated by the cluster transfer-matrix method. A phase diagram with $\langle 2 \rangle$ antiphase, ferromagnetic, incommensurate, and disordered phase is obtained. The bulk uniaxial incommensurate structure modulated in the direction of the competing interactions is found between the $\langle 2 \rangle$ antiphase and the disordered phase. The incommensurate structure near the surface with free and $\langle 2 \rangle$ boundary conditions is studied at different temperatures. Paramagnetic damping at the surface and enhancement of the incommensurate structure in the subsurface region at high temperatures and a new subsurface incommensurate structure modulated in two directions at low temperatures are found.

1. Introduction

The cluster transfer-matrix method was founded as a useful tool for describing commensurate and incommensurate structures in two-dimensional (2D) and three-dimensional (3D) spin lattice models. It is able to describe floating incommensurate structures in two dimensions [1–3] as well as an infinite number of commensurate structures in 3D models [4]. The method yields a phase diagram of the model, free energy, correlation functions, and magnetization as a function of coordinates. As all the calculations are performed in real space, there is a possibility of studying the properties of spatially inhomogeneous systems, for example a lattice with a surface, where the inhomogeneity is localized in one direction, and it is homogeneous in the others.

The cluster transfer-matrix method is a generalized mean-field approximation—it uses auxiliary effective multisite fields that are not directly related to the magnetization or multisite correlation functions of the model, nevertheless, the correlation functions can be calculated from them. In two dimensions, the spatial dependence of the fields in one direction is obtained by simply iterating the effective fields from one lattice row perpendicular to it, to the following one. It is more difficult to get the spatial dependence inside the row, i.e. in the direction perpendicular to the direction of the iteration. Here, the correlation functions of a row of spins interacting by original interactions of the Hamiltonian plus by the spatially dependent effective multisite fields should be found. For that reason the iteration in the systems with uniaxial incommensurate structure is always performed in the direction of the incommensurate modulation.

† E-mail address: fyzisurd@savba.sk

0305-4470/97/124187+12$19.50

The transfer matrix formalism is also used to derive the fermion Hamiltonian in the domain wall theory of commensurate–incommensurate (C–IC) transitions in 2D lattice models [5]. The domain walls in the incommensurate structure are described by world lines of fermions and therefore, the transfer matrices are defined on columns of sites in the direction of the incommensurate modulation, i.e. perpendicular to the transfer matrices used in our method.

It is simple to study surface or subsurface properties in the systems where the surface is perpendicular to the direction of the iteration. In fact, this is always done when the bulk properties of the system are calculated, as the starting values of the effective fields in the iteration procedure play the role of surface boundary conditions. In this case, the most conspicuous properties of the subsurface region appear for the paramagnetic phase near the phase transition line with the incommensurate or ferromagnetic structure. In the first case, the surface effects attenuate with distance from the surface in an oscillatory way, in the latter case, monotonically.

In this paper we study surface and subsurface properties of a 2D system with the surface orientated *parallel* to the incommensurate modulation. Now, the effective fields used in the iteration procedure are functions of distance from the surface and all of them should be stored in the computer memory. Fortunately, far enough from the critical point the surface effects are confined to a relatively narrow region, outside which the effective fields acquire constant bulk values. Thus, the shortest possible distance from the critical point in the parameter space is limited by the computer memory in our calculations.

The cluster transfer-matrix method is related to the mean-field approximation of Jensen and Bak [6] where a nonlinear mapping of site magnetizations instead of effective fields is carried out. There, in distinction to our method, the physically stable solutions are mathematically unstable. The exact nonlinear mapping is possible on lattices without closed loops, such as Cayley tree and Bethe lattice. These lattices are characterized by the site coordination number rather than the dimensionality. This nonlinear mapping technique was applied to various models including Potts [7] Ising [8] and ANNNI model [9]. It is difficult to relate the results for the hierarchical lattices to those for Bravais lattices. Nevertheless, the phase diagram of the ANNNI model on Cayley tree with infinite coordination number [9] bear similar features to that of the 3D ANNNI model.

The ANNNI models, defined on the square lattice and anisotropic antiferromagnetic (AA) model on the triangular lattice, are the most simple 2D models displaying an uniaxial incommensurate structure. There are two competing interactions in both models: ferromagnetic nearest-neighbour (nn) interactions and antiferromagnetic third-nearest-neighbour interactions in the ANNNI model and antiferromagnetic nn and ferromagnetic next-nearest-neighbour (nnn) in the AA model on the triangular lattice. Both models are anisotropic, i.e. two of the third-nn interactions and one or two of the nnn interactions are missing. Both models were investigated by the cluster transfer-matrix approximation and the results were consistent with numerous other approaches such as Monte Carlo calculations, series expansions, cluster variation method, domain wall theory, finite-size scaling [10–13].

The phase diagrams of 2D models are more simple than those in the 3D case. They consist of a small number of commensurate phases and a single region of a floating incommensurate phase. In the ANNNI model, the nn interactions are ferromagnetic and consequently, the rows are ordered ferromagnetically; in the AA model they have a commensurate structure with periodicity of three lattice constants.

Here, we study a natural generalization of the ANNNI model to the triangular lattice. The nn interactions are ferromagnetic and one of the nnn interactions is antiferromagnetic, unlike in the ANNNI model where the antiferromagnetic interaction is between the third-

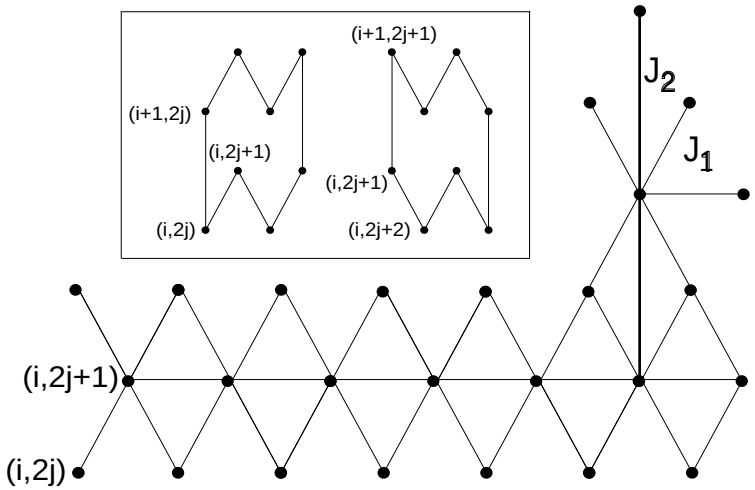

Figure 1. Anisotropic model on a triangular half lattice with two competing interactions. Each spin interacts with six nn spins by J_1 interaction (light lines) and two nnn spins by J_2 interaction (heavy lines). The two types of 2×4 clusters used in the calculation are in the inset. Our zig-zag row encompasses two ordinary rows of the triangular lattice.

nnn. The signs of the interactions of our model are opposite to the above-described AA model. The phase diagram and all other properties are similar to those in the ANNNI model. Hence, it can be expected that the surface effects in the ANNNI model on the square lattice are closely related to those described below.

2. Model and method

We consider an anisotropic ferromagnetic model of Ising spins ($\sigma = \pm1$) on a triangular semi-infinite lattice interacting by nn and one nnn interactions. All the nn interactions of the model are ferromagnetic. Two of the three possible nnn interactions are missing and the remaining one is antiferromagnetic. The triangular lattice with the spin interactions and the clusters used in further calculation are shown in figure 1, where $j = 0, \ldots, \infty$ and $i = -\infty, \ldots, \infty$. We shall calculate the free energy and the local magnetization by using the cluster-matrix method developed by one of us [14].

The cluster-matrix method is based on a subsequent summation of the weight functions $\exp[\beta H(\sigma_i)]$ over the spin variables in the consecutive rows when calculating the partition function. For computational reasons the zig-zag rows shown in figure 1 perpendicular to the nnn interaction are chosen. The lattice surface is perpendicular to the rows and the expected direction of the domain walls. It is put at the column $j = 0$.

Let us write the Hamiltonian of the model

$$H = \sum J_1\sigma_{i,j}(\sigma_{i,j+1} + \sigma_{i,j-1} + \sigma_{i,j+2}) + J_2\sigma_{i,j}\sigma_{i+1,j}$$

as a sum of energies of the 2×4 clusters

$$H = \sum_{i,j}[G_{i,2j} + G'_{i,2j+1}].$$

We use two types of the 2×4 clusters, that are shifted by one lattice constant and can be transformed into each other by translation and rotation by an angle of 180° in the plane of the lattice. They are shown in the inset of figure 1.

The energy of the bulk cluster of the first type is

$$G_{i,2j} = J_1\Big[\sigma_{i,2j+1}\Big(\frac{\sigma_{i,2j}}{6}+\frac{\sigma_{i,2j+2}}{6}+\frac{\sigma_{i,2j+3}}{3}+\frac{\sigma_{i+1,2j}}{3}+\frac{\sigma_{i+1,2j+2}}{3}\Big) +\sigma_{i+1,2j+2}\Big(\frac{\sigma_{i+1,2j+1}}{6}+\frac{\sigma_{i+1,2j+3}}{6}+\frac{\sigma_{i+1,2j}}{3}+\frac{\sigma_{i,2j+3}}{3}\Big) +\frac{\sigma_{i,2j+2}\sigma_{i,2j+3}}{6}+\frac{\sigma_{i+1,2j}\sigma_{i+1,2j+1}}{6}\Big]+J_2\Big[\frac{\sigma_{i,2j}\sigma_{i+1,2j}}{4} +\frac{\sigma_{i,2j+1}\sigma_{i+1,2j+1}}{4}+\frac{\sigma_{i,2j+2}\sigma_{i+1,2j+2}}{4}+\frac{\sigma_{i,2j+3}\sigma_{i+1,2j+3}}{4}\Big] \tag{1}$$

where J_1 is the nn interaction and J_2 is the nnn interaction and $j = 1, 2, \ldots, \infty$. The terms in (1) are divided by the number of appearances of the particular bond in different overlapping clusters. The expression for the energy of the cluster of the second type denoted by $G'_{i,2j+1}$ can be found by interchanging $i \leftrightarrow i+1$ and $2j \rightarrow 2j+1$ on the right-hand side of (1). The denominators in (1) are different in the expressions for the energies $G_{i,0}$ and $G'_{i,1}$ of the surface clusters, because the translational symmetry is broken here.

The evaluation of the partition function

$$Z = \sum_{\{\sigma_i\}} \exp[\beta H(\sigma_i)]$$

can be transformed into the calculation of the numbers λ_i appearing as normalization factors in the iterative procedure for auxiliary functions Ψ_i

$$\sum_{S_i} \Psi_i(S_i) T_i(S_i, S_{i+1}) = \lambda_i \Psi_{i+1}(S_{i+1}) \tag{2}$$

starting from an appropriate function $\Psi_1(S_1)$ [1–3]. (S_i denotes a row variable $S_i \equiv \{\sigma_{i,0} \ldots, \sigma_{i,2j}, \sigma_{i,2j+1}, \sigma_{i,2j+2} \ldots\}$ and $T_i(S_i, S_{i+1}) = \exp[\beta \sum_{j=0}^{j=+\infty}(G_{i,2j} + G'_{i,2j+1})]$.) $Z = \prod_{i=0}^{\infty} \lambda_i$.

Unfortunately, each of the auxiliary functions $\Psi_i(S_i)$ acquires an infinite number of values and an approximation should be done to perform the summation on the left-hand side of (2).

Assuming an asymptotic behaviour of correlation functions already at distances exceeding the cluster size, we can try to factorize $\Psi_i(S_i)$ in the same way as the function $T_i(S_i, S_{i+1}) = \prod_{j=0}^{\infty} \exp(G_{i,2j}) \exp(G'_{i,2j+1})$, i.e.

$$\Psi_i(S_i) \simeq \prod_{j=0}^{\infty} \Psi_{i,2j}(s^k_{i,2j}) \Psi'_{i,2j+1}(s^k_{i,2j+1}) \tag{3}$$

where $s^k_{i,l}$ denotes a set of site variables of a finite row cluster $s^k_{i,l} = (\sigma_{i,l}, \ldots, \sigma_{i,l+k})$ and $\Psi_{i,2j}(s^k_{i,2j})$, $\Psi'_{i,2j+1}(s^k_{i,2j+1})$ are the cluster auxiliary functions acquiring a finite number of values.

The number k characterizes the order of the approximation and was taken to be equal to 4 which is the width of the clusters in (1) (figure 1).

The logarithms of the values of the cluster auxiliary function for different cluster configuration represent the above-mentioned multisite effective fields. As the functions are defined on finite clusters, only short-range effective interactions are taken into account in our approximation.

Substituting (3) into (2), we obtain a relation between the known functions $\Psi_{i,2j}$, $\Psi'_{i,2j+1}$ found in the preceding iteration step and the new functions $\Psi_{i+1,2j}$, $\Psi'_{i+1,2j+1}$. The expression for $\Psi_{i+1,2j}$, $\Psi'_{i+1,2j+1}$ in terms of $\Psi_{i,2j}$, $\Psi'_{i,2j+1}$ can be found by a partial summation of the both sides of (2). This problem is one-dimensional (1D) and the partial

summation can be done exactly—again by the technique of auxiliary functions as shown in detail in [1–3, 14]. In contrast to the previous calculations on infinite lattices, equation (2) has no translational symmetry in the row direction due to the presence of the surface and the equation should be solved for all $\Psi_{i+1,2j}$, $\Psi'_{i+1,2j+1}$, $j = 0, \ldots, \infty$. In practice, the cluster auxiliary functions would converge to their bulk values fastest if we were far enough from the continuous IC–C phase transition. We confined ourselves to the distances from the IC–C phase transition line where the number of the cluster auxiliary functions taken into account did not exceed $j = 400$.

In the paramagnetic and ferromagnetic phase $\Psi_{i,2j}$, $\Psi'_{i,2j+1}$ do not depend on i, in the $\langle 2 \rangle$ antiphase consisting of zig-zag rows with alternating magnetization, $\Psi_{i,2j}$, $\Psi'_{i,2j+1}$ are periodic functions of i with period of two. In the incommensurate phase, their period is a continuous function of the interaction constants. The functions $\Psi_{i,2j}$, $\Psi'_{i,2j+1}$ are j independent in the bulk, i.e. the row structure is ferromagnetic or paramagnetic in all phases. Nevertheless, they are strongly spatially modulated near the surface which leads to the areas of reversed magnetization.

From our knowledge of the auxiliary functions Ψ and Ψ', it is possible to find the site magnetizations. We have

$$\langle \sigma_{i,l} \rangle = \sum_{S_i} \prod_j \Psi_{i,2j}(s^k_{i,2j}) \Psi'_{i,2j+1}(s^k_{i,2j+1}) \sigma_{i,l} \tilde{\Psi}_{i,2j}(s^k_{i,2j}) \tilde{\Psi}'_{i,2j+1}(s^k_{i,2j+1}) \qquad (4)$$

where $\tilde{\Psi}'$, $\tilde{\Psi}'$ are the functions that are calculated by the same iteration procedure as in (2) but in the opposite direction.

3. Results and discussion

The calculations have shown that the anisotropy model with competing nn and nnn interactions on a triangular lattice can be found in one of the four phases: disordered paramagnetic, commensurate $\langle 2 \rangle$ antiphase, ferromagnetic, and the incommensurate one lying between them.

The phase diagram of the model, shown in figure 2, is similar to the phase diagram of the 2D ANNNI model on the square lattice [2, 10, 11]. Near the multiphase point $J_1/J_2 = 1$ the disordered phase should persist to $T = 0$ in the form of an extremely narrow strip. Unfortunately, by using our method it is not possible to verify this fact at very low temperatures and the direct phase transition between the ferromagnetic and the incommensurate phase cannot be excluded. On the other hand, we found no signs confirming the opposite case. For $J_1/J_2 \to 0$ the incommensurate phase seems to be stable down to the point $T = 0$. The IC-disorder phase transition line appears to tend to a Lifshitz point at the ferrodisorder phase transition line but at the close vicinity of it, it turns abruptly down and apparently meets it at $T = 0$. It is seen that a less careful numerical treatment of the problem could lead to an erroneous confirmation of the Lifshitz point in 2D ANNNI model.

When we put $J_2 = 0$, the exactly solvable ferromagnetic Ising model on the triangular lattice with a critical temperature of $T_c = 3.732\ldots$ is restored. Our method yields $T_c = 3.64$. We believe that the comparison of these two values suggests the accuracy of the whole phase diagram shown in figure 2.

The interaction constants and temperature in all further presented results are localized in the areas denoted by two short bars in the incommensurate region of the phase diagram near the phase transition lines with the disordered paramagnetic phase and $\langle 2 \rangle$ antiphase, respectively. At higher temperatures the bulk magnetization is of a sinusoidal shape. At lower temperatures the structure consists of strip-like $\langle 2 \rangle$ antiphase domains. Their width

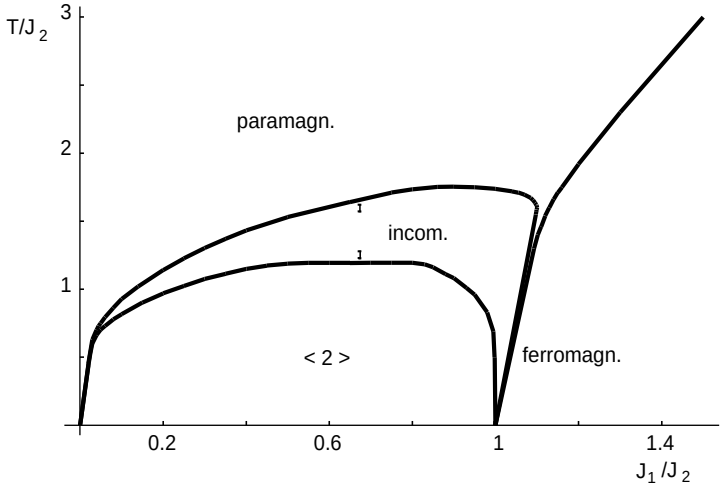

Figure 2. Phase diagram of the model. The two short bars (at $J_1/J_2 = 0.5$, $T/J_2 = 1.241, 1.47$) show the parameter regions of the calculations presented in figures 3–8.

is growing to infinity with temperature approaching the IC–C phase transition line. The bulk structures can be seen in a depth of more than 400 columns from the surface in the following figures.

We consider two different boundary conditions at the surface: the free boundary condition (FBC) and the $\langle 2 \rangle$ antiphase boundary condition (ABC). In our approach the boundary condition is given by the starting values $\Psi_{i,0}$ of the auxiliary function. For FBC all values of the auxiliary function on the surface are taken to be equal to unity. The ABCs can be simulated by the values of the cluster auxiliary function deep in the bulk of the $\langle 2 \rangle$ structure at low temperature. Actually, they have been taken as an output of calculation at $J_1/J_2 = 0.5$, $T/J_2 = 0.1$ for $j = 600$.

The site magnetizations at every second zig-zag row and at the first 480 subsurface columns for $T/J_2 = 1.47, 1.252, 1.247, 1.241$ are shown in figures 3(a)–(d). All these figures are calculated for the FBC. In figure 4, the magnetization along the rows of sites with maximum absolute value of magnetization as a function of distance from the surface is shown.

As expected, the amplitude of the sinusoidal magnetization at the surface is diminished by the absence of interactions for FBC at the temperature $T/J_2 = 1.47$, close to the paramagnetic structure. This suppression is replaced by an enhancement of the incommensurate waves of magnetization in the narrow subsurface region (figure 3(a)). The presence of the surface affects, approximately, only the first 60 columns at this temperature. A similar increase of the magnetization profile near the surface was found for the semi-infinite ferromagnetic Ising model [15].

The situation is different for temperatures near the IC–C phase transition where wide 1D domains of $\langle 2 \rangle$ structure bounded by domain walls perpendicular to the nnn J_2 interaction J_2 occur in the bulk. Two neighbouring domains differ by a phase shift of π (figures 3(b)–(d)). Near the surface, the strip-like bulk domains become modulated, as well, and incommensurate domains are formed in the direction perpendicular of the nnn interaction. By approaching the IC–C phase transition line (lowering the temperature) the region of the biaxial incommensurate structure becomes wider and its depth changes linearly with

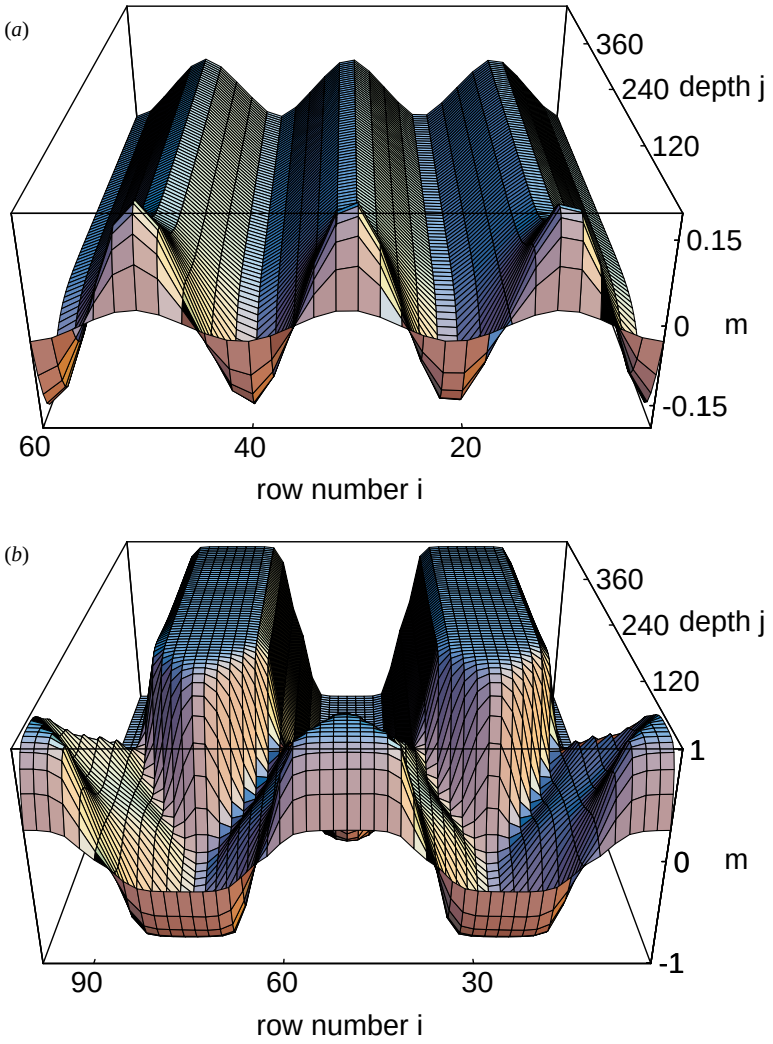

Figure 3. (*a*) Site magnetizations $m_{i,j} = \langle \sigma_{i,j} \rangle$ at the first 480 subsurface columns ($j = 1, \ldots, 480$) for $T/J_2 = 1.47$, $J_1/J_2 = 0.5$ and FBC. (*b*) Site magnetizations $m_{i,j}$ at the first 480 subsurface columns for $T/J_2 = 1.252$, $J_1/J_2 = 0.5$ and FBC. (*c*) Site magnetizations $m_{i,j}$ at the first 480 subsurface columns for $T/J_2 = 1.247$, $J_1/J_2 = 0.5$ and FBC. (*d*) Site magnetizations $m_{i,j}$ at the first 480 subsurface columns for $T/J_2 = 1.241$, $J_1/J_2 = 0.5$ and FBC.

(This figure can be viewed in colour in the electronic version of the article; see `http://www.iop.org/EJ/welcome`)

temperature, as shown in figure 5. Extrapolating the linear plot to the temperature of the phase transition $T_{\mathrm{IC-C}} = 1.1876$, the width of the biaxially modulated structure at the critical point is found approximately equal to 1300 columns.

Figures 6 and 7 show that the influence of the boundary condition is small. The change from FBC to ABC affects only the first few subsurface columns. The phase of the $\langle 2 \rangle$ structure is fixed at the surface, but it does not influence the phase in the bulk that changes quite freely at the domain walls. The structure perpendicular to the surface is also unaffected.

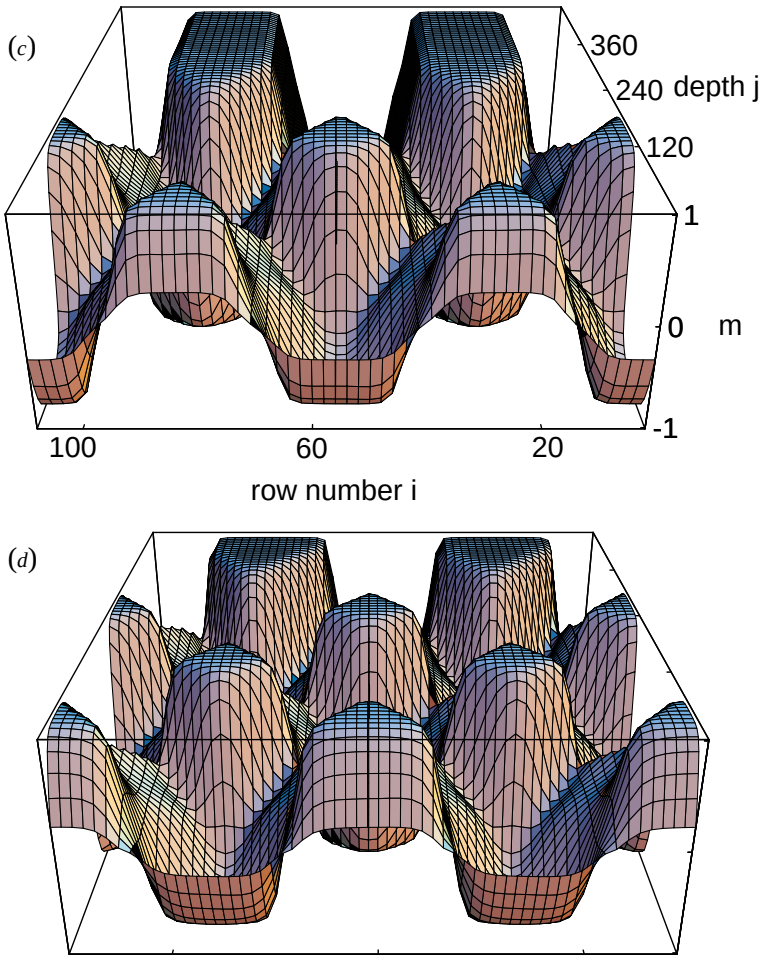

Figure 3. (Continued)

(This figure can be viewed in colour in the electronic version of the article; see `http://www.iop.org/EJ/welcome`)

Here it is necessary to note that the incommensurate structures in 2D lattice models are floating, i.e. they can be shifted freely with respect to the underlying lattice. Thus, not only is the total magnetization of an incommensurate structure at a vanishing magnetic field equal to zero, but also the local one is. Typically, the mean-field approximations spontaneously break the symmetry of the model in the ordered phase. In our case the iteration technique also involves a self-consistent procedure characteristic for a mean-field treatment that fixes the structure at one position. Then, the incommensurate structure is represented by a wave-like site dependence on the magnetization. To obtain results corresponding to the exact summation of the partition function, we have to further sum over all positions of the floating structure. In this case the site magnetizations would be equal to zero and only the pair spin correlation function would reflect the incommensurate space modulation.

The cluster auxiliary functions $\Psi_{i,2j}$, $\Psi'_{i,2j+1}$ are the direct output of the iteration procedure and in the bulk behave similarly to the magnetization shown in the previous figures. In the low-temperature incommensurate structure, they form 1D strip-like domains

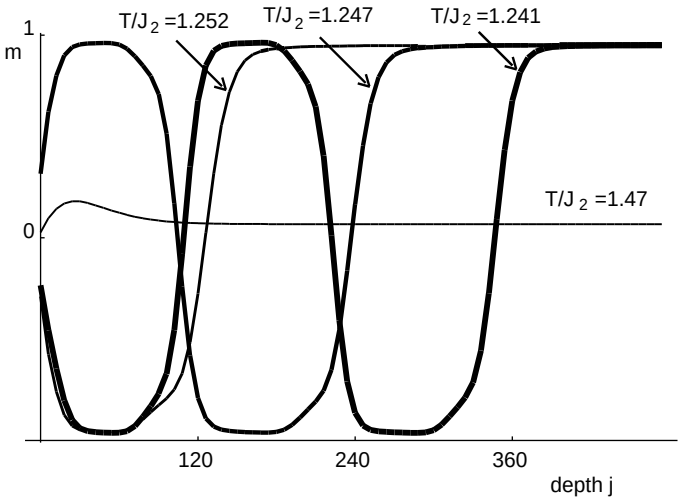

Figure 4. Site magnetizations $m_{i,j}$ in the direction perpendicular to the surface as a function of the column number j at $T/J_2 = 1.241$ (the heaviest curve), 1.247, 1.252, 1.47 (the lightest curve) and $J_1/J_2 = 0.5$ for FBC. The curves follow one of ridges of the structures in figures 3(*a*)–(*d*).

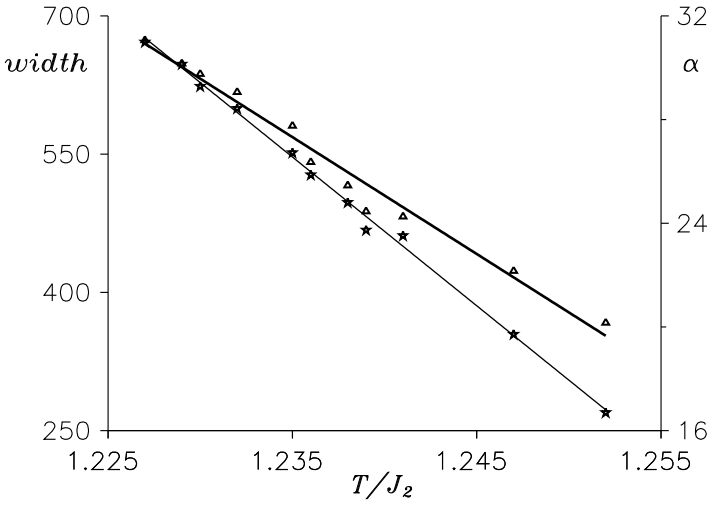

Figure 5. Width of the surface affected region (stars) and angle α between of the bulk auxiliary-function domain wall and the domain wall near the surface (triangles).

possessing the symmetry of $\langle 2 \rangle$ phase. Near the surface the domains bend in the opposite direction to the direction of the iteration.

This situation is shown in figure 8, where one of the 64 values of the cluster auxiliary function $\Psi_{i,2j}$ at subsurface lattice sites is plotted. The direction of the iteration is from left to right, i.e. the domains are bent backwards. It looks like there is a friction between the auxiliary-function structures and the surface when the space evolution of the auxiliary function is calculated by the iteration procedure.

The domains are bent but near the surface they are again straight. The bending angle between the direction of the bulk and surface domain increases when approaching the critical

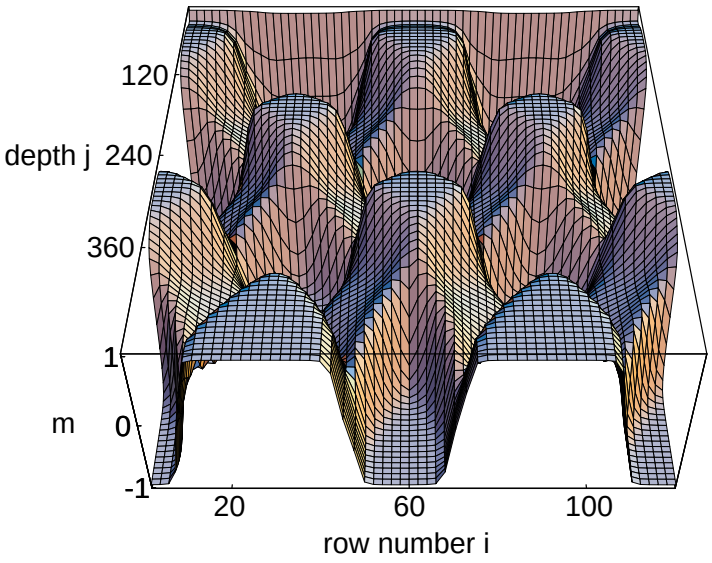

Figure 6. Site magnetizations $m_{i,j}$ at the first 480 subsurface columns for $T/J_2 = 1.241$, $J_1/J_2 = 0.5$ and ABC.

(This figure can be viewed in colour in the electronic version of the article; see `http://www.iop.org/EJ/welcome`)

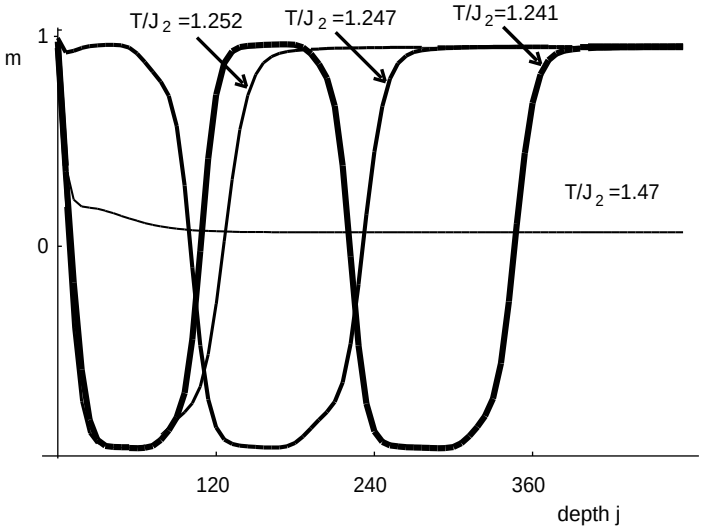

Figure 7. Site magnetizations $m_{i,j}$ in the direction perpendicular to the surface as a function of the column number j at $T/J_2 = 1.241$ (the heaviest curve), 1.247, 1.252, 1.47 (the lightest curve) and $J_1/J_2 = 0.5$ for ABC. The curves follow one of the ridges of the structure in figure 6.

line as shown in figure 5. At the critical temperature, the angle tends to 45°.

The magnetization is calculated from equation (4) which involves two auxiliary function which are iterated in opposite directions and therefore their surface parts are bent in the opposite sense. The surface incommensurate structure is in fact their interference pattern

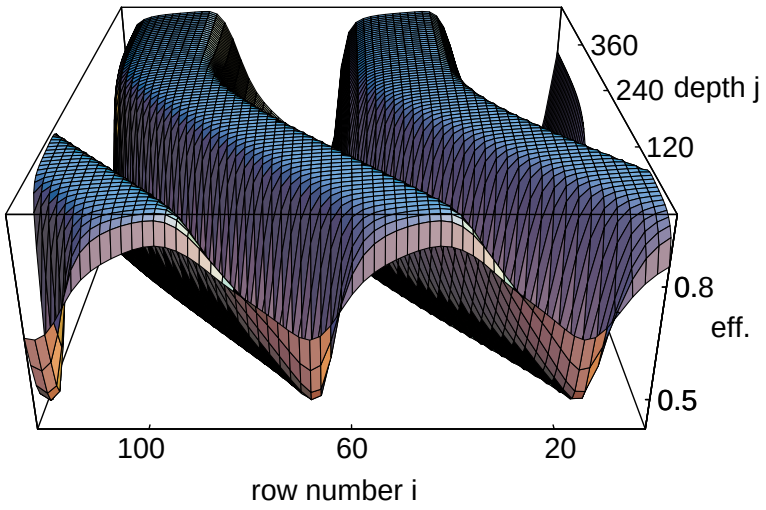

Figure 8. Cluster auxiliary function $\Psi_{i,j}$ at the first 480 subsurface columns for $T/J_2 = 1.247$, $J_1/J_2 = 0.5$ and FBC. Direction of iteration is from left to right.

(This figure can be viewed in colour in the electronic version of the article; see `http://www.iop.org/EJ/welcome`)

and the resulting modulation of the magnetization has a 2D character.

As the bending angle of the auxiliary-function domains is between 0° and 45° the 2D magnetization domains are oblong at higher temperatures and become square-like near the phase transition line. On the other hand, if the linear extrapolation is applicable up to the critical line, the width of the bulk domains becomes infinite while the width of the surface region remains finite. Thus, the subsurface structure should in fact disappear at the phase transition.

The width of the subsurface structure was measured as a distance from the surface to the point of the maximum curvature of the bent domain wall.

In conclusion, the influence of the surface on the incommensurate structure of an anisotropic Ising model on a triangular lattice was investigated by the cluster transfer-matrix method. The uniaxial incommensurate structure in a finite region near the surface changes its character and becomes biaxial. The width of the biaxially modulated structure seems to be finite at critical temperatures. Formation of the biaxial structure can be interpreted as an interference pattern of two auxiliary-function wave-like structures.

From a more physical point of view, it can be seen as a result of a misfit between the bulk structure with longer periodicity than that of the surface structure due to the absence of a part of the interaction at the surface that is equivalent to an effective increase in temperature.

Acknowledgment

This work was supported by Slovak Grant Agency, grant no 2/4109/97.

References

[1] Šurda A 1991 *Physica* **178A** 332

[2] Karasová I and Šurda A 1993 *J. Stat. Phys.* **70** 675
[3] Pajerský P and Šurda A 1994 *J. Stat. Phys.* **76** 1467
[4] Šurda A 1996 *Commensurate and incommensurate structures in 3D ANNNI model* (to appear)
[5] den Nijs M 1992 *Phase Transition and Critical Phenomena* vol 12 (New York: Academic)
[6] Jensen M H and Bak P 1983 *Phys. Rev.* B **27** 6853
[7] Monroe J L 1996 *J. Phys. A: Math. Gen.* **29** 5421
[8] Mélin R, Anglès d'Auriac J C, Chandra P and Douçot B 1996 *J. Phys. A: Math. Gen.* **29** 5773
[9] Yokoi C S O, de Oliveira M J and Salinas S R 1985 *Phys. Rev. Lett.* **54** 163
[10] Selke W 1988 *Phys. Rep.* **170** 213
[11] Selke W 1992 *Phase Transition and Critical Phenomena* vol 15 (New York: Academic)
[12] de Queiroz S L A and Domany E 1995 *Phys. Rev.* E **52** 4768
[13] Kitatani H and Oguchi T 1988 *J. Phys. Soc. Japan* **1344**
[14] Šurda A 1991 *Phys. Rev.* B **43** 908
[15] Czerner P and Ritschel U 1996 Magnetization profile in the $d = 2$ semi-infinite Ising model and crossover between ordinary and normal transition *SISSA-preprint* cond-mat 969120